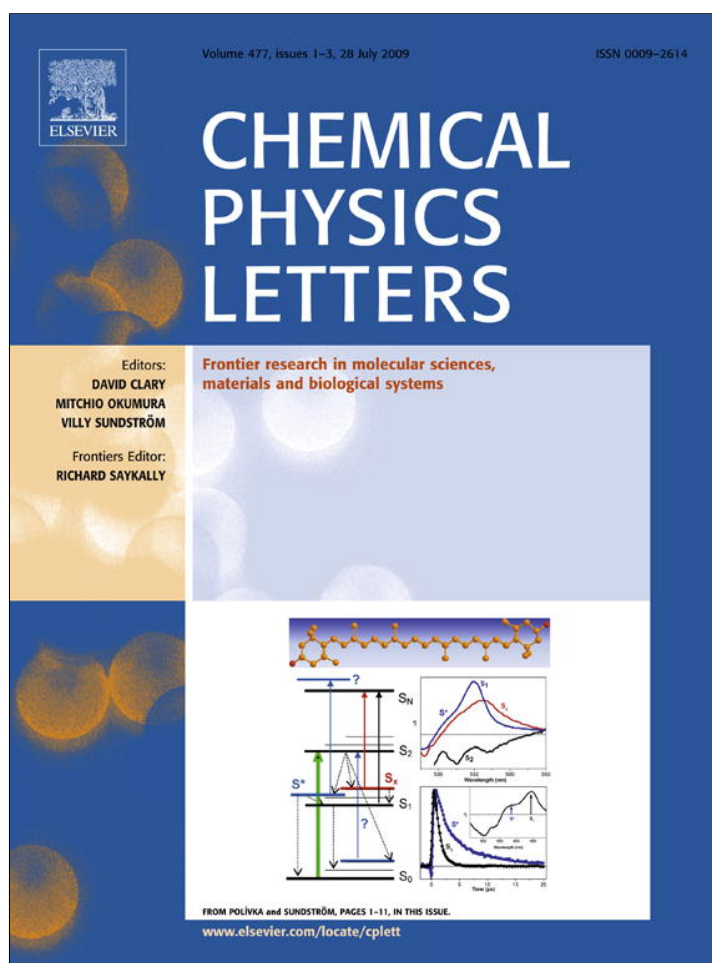


Provided for non-commercial research and education use.
Not for reproduction, distribution or commercial use.



This article appeared in a journal published by Elsevier. The attached copy is furnished to the author for internal non-commercial research and education use, including for instruction at the authors institution and sharing with colleagues.

Other uses, including reproduction and distribution, or selling or licensing copies, or posting to personal, institutional or third party websites are prohibited.

In most cases authors are permitted to post their version of the article (e.g. in Word or Tex form) to their personal website or institutional repository. Authors requiring further information regarding Elsevier's archiving and manuscript policies are encouraged to visit:

<http://www.elsevier.com/copyright>



Contents lists available at ScienceDirect

Chemical Physics Letters

journal homepage: www.elsevier.com/locate/cplett

Mechanism for giant electrooptic response of excitons in porphyrin J-aggregates: Molecular rearrangement model

Tomohiro Katsumata^a, Kazuaki Nakata^a, Takashi Ogawa^a, Katsunori Koike^a, Takayoshi Kobayashi^{c,d}, Eiji Tokunaga^{a,b,*}^a Department of Physics, Faculty of Science, Tokyo University of Science, 1-3 Kagurazaka, Shinjuku-ku, Tokyo 162-8601, Japan^b Research Center for Green Photo-Science and Technology, Tokyo University of Science, 1-3 Kagurazaka, Shinjuku-ku, Tokyo 162-8601, Japan^c Department of Applied Physics and Chemistry, Institute for Laser Science, University of Electro-Communications, 1-5-1 Chofugaoka, Chofu, Tokyo 182-8585, Japan^d International Cooperative Research Project (ICORP), Japan Science and Technology Agency, 4-1-8 Honcho, Kawaguchi, Saitama 332-0012C, Japan

ARTICLE INFO

Article history:

Received 20 March 2009

In final form 19 June 2009

Available online 24 June 2009

ABSTRACT

We propose possible mechanisms for the highly enhanced electrooptic response by formation of J-aggregates observed for porphyrin molecules. For J-aggregates, the signal intensity deviates from the quadratic dependence on the electric field to show saturation behavior for a high field, while that for monomers obeys the quadratic dependence, as expected for the Kerr response. This phenomenon can be explained by the molecular rearrangement model, where the dipole–dipole interaction energy is modified by field-induced change in the angle between the molecular transition dipole moment and the aggregation axis. A possible contribution of charge-transfer states to the electrooptic response is also evaluated.

© 2009 Elsevier B.V. All rights reserved.

1. Introduction

For optical communication and optical information processing technology, materials with large optical nonlinearity are highly demanded for electron–photon and photon–photon information conversion. One of the solutions is the use of excitonic nonlinearity, for which Frenkel excitons in J-aggregates are candidates owing to sharp resonance and a large transition dipole moment. We have reported that the difference in the static polarizability, $\Delta\alpha$, between the excited and ground states is 70 times larger for J-aggregates than for monomers [1]. This is a remarkable result, but the mechanism of the extraordinary enhancement of electrooptic response has since been left to be explained.

There is a model to explain that $\Delta\alpha$ scales with the coherent aggregation number N_c , the size of a meso-aggregate [2–4]. From this model, it is concluded that TPPS J-aggregates have the coherent size as large as 70 molecules. However, other experimental facts indicate a smaller number (from 5 to 20) of size [5–10]. In addition, this model takes into account only two levels (the ground and single exciton states), where $\Delta\alpha$ is always negative, in contradiction with the positive values for $\Delta\alpha$ in most of experiments. In order to explain these positive values, one should take into account higher excited states, i.e., more than the two levels. In such a realistic model, it is discussed that there is no enhancement in $\Delta\alpha$ due

to N_c if the two-exciton state is also taken into account [11]. As a mechanism for electrooptic response in molecular crystals, it is also proposed that the coupling between charge-transfer (CT) and the Frenkel states is crucial for the enhancement of $\Delta\alpha$, and this model has accounted for the experimental electroabsorption spectra in polyacene crystals [12–14].

In the present Letter, we propose a new model for explaining the large enhancement for $\Delta\alpha$ by formation of J-aggregates. It is the molecular rearrangement model, where an electric-field-induced change in the angle between the molecular transition dipole moment and the bonding axis of the meso-aggregate is responsible for the giant electrooptic response. In order to verify this model, we have investigated the dependence of the signal on the frequency and the electric-field strength to show that the experimental results are consistent with this model.

2. Experimental

J-aggregates and monomers of tetraphenyl porphyrin tetrasulfonic acid (TPPS) dispersed in polyvinylalcohol (PVA) thin films on glass substrates were prepared with the method depicted in Ref. [1]. Prior to the preparation of sample films, an array of 8 interdigitated aluminum electrodes, each with a width of 0.5 mm separated by gaps of 0.5 mm, was deposited on the slide glass by vacuum evaporation.

White light from a xenon-lamp (Hamamatsu, L2273) was collimated after focused through a 200- μm pinhole and then loosely focused on the sample to cover the multiple electrode gaps. An ac electric field of $F_{\text{ext}} = F_0 \sin(2\pi ft)$ with $F_0 \approx 10^6$ V/m and

* Corresponding author. Address: Department of Physics, Faculty of Science, Tokyo University of Science, 1-3 Kagurazaka, Shinjuku-ku, Tokyo 162-8601, Japan. Fax: +81 3 5261 1023.

E-mail address: eiji@rs.kagu.tus.ac.jp (E. Tokunaga).

$f = 20\text{--}25\,000$ Hz was applied between the electrodes by using a function generator (NF, 1956 multifunction synthesizer) combined with a high-voltage amplifier (Matsusada, HEOPT-5B20) to detect the field-induced absorbance change through a spectrometer with a multichannel lock-in amplifier [15]. f was extended to a value 10 times as large as that used in the preceding report [1]. The absorbance changes due to the Pockels and Kerr effects were detected at the modulation frequency f and its second harmonic $2f$, respectively. Here we focused on the Kerr response, for which $\Delta\alpha$ was deduced from the red shift of the B band for both monomer and J-aggregates. In order to study the dependence of the signal on the electric-field strength, the field amplitude was slowly modulated with a period of 1000 s, while full transmission change spectra were taken for every 10 s with $f = 235$ Hz.

The method of data analysis followed Ref. [1]. Because the conventional spin-coating method was used, the axes of the J-aggregates were two-dimensionally oriented parallel to the film plane. The external electric field F_{ext} was within the film plane. The local field F_{loc} was estimated by the Lorentz field with the dielectric constant ε as

$$F_{\text{loc}} = \frac{\varepsilon + 2}{3} F_{\text{ext}}, \quad (1)$$

where $\varepsilon = 5.9$ for PVA. The absorption change can be written as [1,16]

$$\Delta A = \left\{ A_0 |\Delta\mu|_f \frac{\partial A}{\partial E} \right\} |F_{\text{loc}}| + \left\{ B_0 \Delta\alpha \frac{\partial A}{\partial E} + C_0 |\Delta\mu|_{2f}^2 \frac{\partial^2 A}{\partial E^2} \right\} |F_{\text{loc}}|^2, \quad (2)$$

where A_0 , B_0 , and C_0 are constants depending on the degree of molecular orientation. These values can be estimated by comparing $|\Delta\mu|_f = |\sum \Delta\mu_i|/N$ determined from the Pockels effect with $|\Delta\mu|_{2f} = \sqrt{\sum |\Delta\mu_i|^2}/N$ from the Kerr effect, where N denotes the number of monomers or J-aggregates.

3. Results

Fig. 1 shows an absorption spectrum of TPPS J-aggregates, a typical electroabsorption spectrum, and the fitting curve calculated from the first derivative of the absorption spectrum.

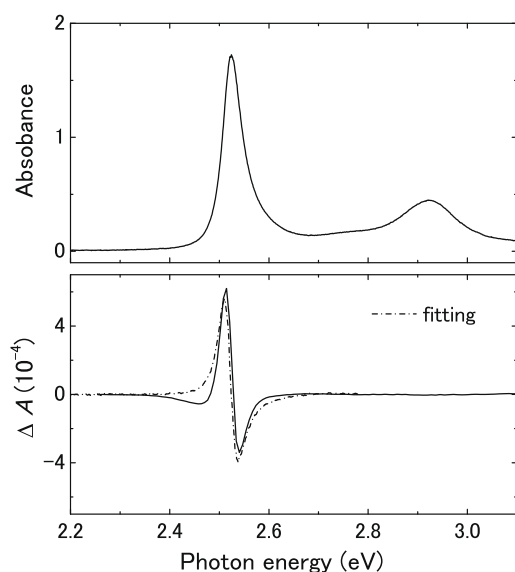


Fig. 1. Top: absorption spectrum of TPPS J-aggregates. Bottom: typical electroabsorption spectrum (solid curve) taken at $2f$ with $f = 235$ Hz and $F_{\text{ext}} = 2.1 \times 10^6$ V/m for 10 s and the fitting curve (dash-dotted curve) calculated from the first derivative of the absorption spectrum.

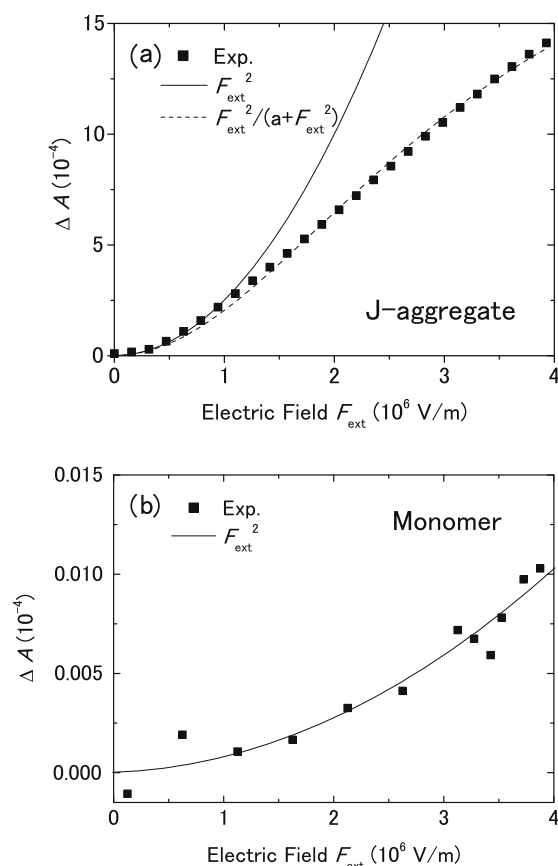


Fig. 2. The signal intensity (peak absorption change in the B band due to the red shift at $2f$) as a function of the external electric field for aggregates (a) and for monomers (b) at $f = 235$ Hz. (a) J-aggregates: the fitting curves are proportional to F_{ext}^2 (solid curve) and $F_{\text{ext}}^2/(a + F_{\text{ext}}^2)$ (dashed curve). In the unit of 10^6 V/m for F_{ext} , $a = 10.3$. The amplitude F_{ext} for the AC electric field was periodically modulated between 0 and 4×10^6 V/m at the period of 1000 s. The signal spectra were stored every 10 s with a time constant of 3 s for the multilock-in detection. The data over 3 periods were averaged. (b) Monomers: the fitting curve is proportional to F_{ext}^2 (solid curve).

Fig. 2 shows the electric-field dependence of the signal intensity, i.e., the change in the peak absorption of the B band due to the red shift. For the J-aggregates, the signal intensity deviates from the quadratic dependence on F_{ext} for higher F_{ext} , while that for the monomers obeys the quadratic dependence. This dependence was reproduced for periodic cycles of increasing and decreasing electric field. Fig. 3 shows the electric-field dependence

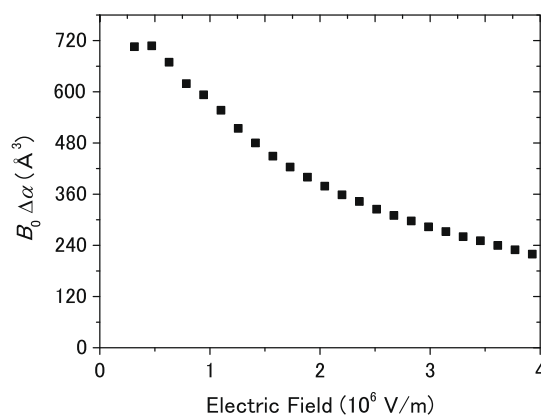


Fig. 3. Electric-field dependence of $B_0 \Delta\alpha$, which is proportional to $\Delta A/F_{\text{ext}}^2$, for aggregates obtained from the results in Fig. 2a.

of $B_0\Delta\alpha$, which is proportional to $\Delta A/F_{\text{ext}}^2$, for the J-aggregates obtained from the results in Fig. 2a.

Fig. 4 shows the modulation frequency (f) dependence of the ratio of $\Delta\alpha$ for the J-aggregates to that for the monomers. Three typical patterns for the dependence are shown in (a)–(c). $\Delta\alpha$ for the monomers has no frequency dependence, as shown in (d).

No significant change in the absorbance was observed before and after the electroabsorption experiments for all the samples. Thus, there was no detectable degradation (such as bleaching effect) in the samples during the experiments.

Table 1 summarizes the results for the present experiments and those for the preceding paper [1]. Although the experimental values for $\Delta\alpha$ are distributed due to sample dependence both for the monomers and the aggregates, the ratio of $\Delta\alpha_{\text{agg}}$ to $\Delta\alpha_{\text{mon}}$

(enhancement factor) ranges from 500 (low field) to 15 (high field). The ratio of 60–80 reported in Ref. [1] falls within this range.

In Table 1, errors in Ref. [1] are corrected. In Ref. [1], $F_{\text{loc}} = [(\epsilon + 2)/(3\epsilon)]F_{\text{ext}}$ was used. Therefore $\Delta\alpha$ was overestimated because F was underestimated. $\Delta\mu$ was also in error because the conversion factor was taken as 1 Debye = 3×10^{-31} C m, while the true one is 1 Debye = 3.34×10^{-30} C m. The values for $\Delta\mu$ in Ref. [1] was doubly overestimated due to the errors in the conversion factor and the local field. The reestimated values in the B-band are as follows. $\Delta\alpha$ for J-aggregates is 570–1100 \AA^3 while $\Delta\alpha$ for monomer is 10–14 \AA^3 . $|\Delta\mu|_{2f}$ for J-aggregates is less than 0.17 D while $|\Delta\mu|_{2f}$ for monomer is less than 0.017 D. $|\Delta\mu|_f$ for J-aggregates is less than 0.009 D while $|\Delta\mu|_f$ for monomer is less than 0.0005 D.

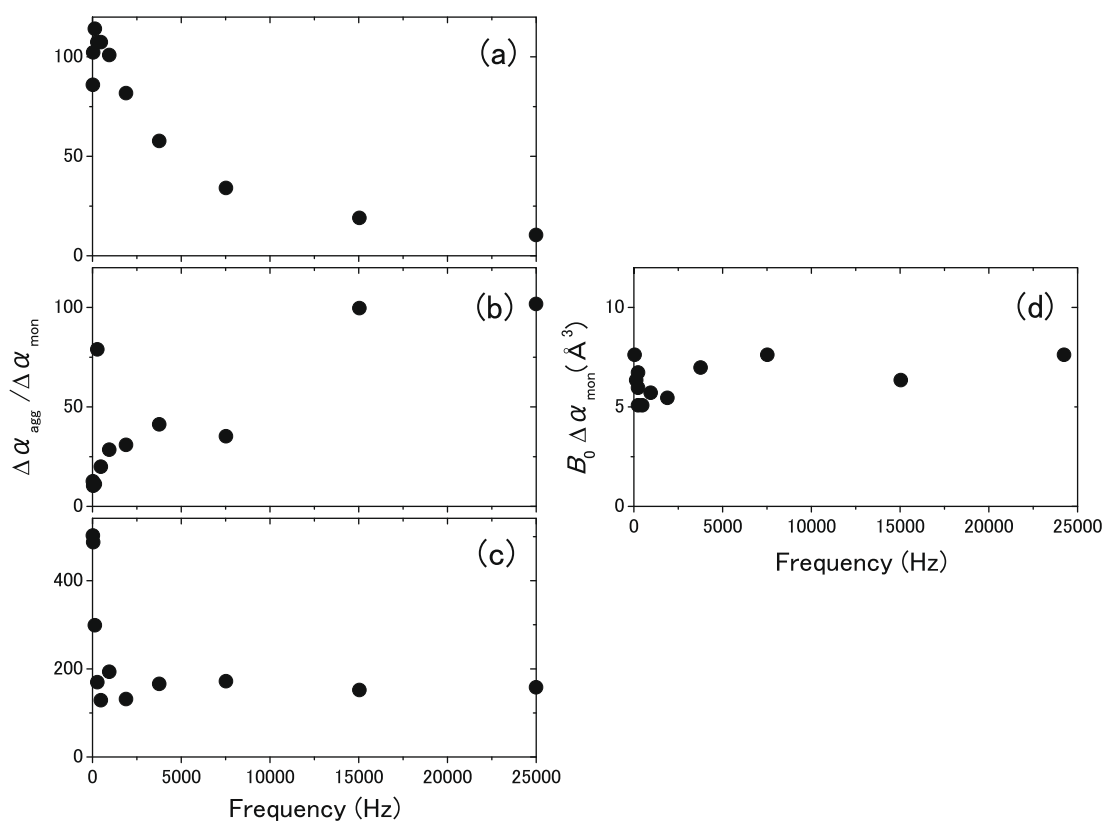


Fig. 4. Modulation frequency dependence of the ratio of $\Delta\alpha$ for J-aggregates to that for monomers. Three typical patterns of dependence are shown in (a)–(c). $\Delta\alpha$ for monomers in (d) does not have the frequency dependence. B_0 in Eq. (2) is assumed to have the same value for both monomers and J-aggregates. $F_{\text{ext}} = 2.5 \times 10^6$ V/m for (a) and (b), 2.1×10^6 V/m for (c), and 2.9×10^6 V/m for (d).

Table 1

Stark parameters of the TPPS J-aggregate and monomer.

Work	B-band	$B_0\Delta\alpha$ (\AA^3) ^a	
		High field ($>3 \times 10^6$ V/m)	Low field ($<2 \times 10^6$ V/m)
Present paper	Aggregate	100–300	200–2000
	Monomer	4–7	4–7
Preceding paper [1]	Aggregate	280 (3.1×10^6 V/m)	
	Monomer	5 (3.1×10^6 V/m)	

^a $\Delta\alpha$ is a diagonal component of the $\Delta\alpha$ tensor. For aggregate, $\Delta\alpha = \text{Tr}\Delta\alpha$ while for monomer $2\Delta\alpha = \text{Tr}\Delta\alpha$ [1]. B_0 ranges from 7/20 to 1/2 for monomer and from 1/4 to 1/2 for aggregate. The local field factor is taken as $g = (\epsilon + 2)/3 = 2.63$. The values without this correction are given by $g^2 B_0\Delta\alpha$. The modulation frequency is in the range of 100 Hz $< f < 1$ kHz, where no substantial frequency dependence was observed.

4. Models and discussion

4.1. Molecular rearrangement model

The transition dipole–transition dipole interaction energy J is expressed by Ref. [17]

$$J = \frac{M^2}{4\pi\epsilon_b r^3} (1 - 3 \cos^2 \theta), \quad (3)$$

where M is the transition dipole moment of the molecule, r is the intermolecular distance, ϵ_b is the background permittivity, and θ is the angle between the molecular transition dipole moment and the intermolecular bonding (aggregation) axis. J determines the absorption energy of the J-aggregates such that the energy shift from the monomer energy is given by $2J$. It depends strongly on the molecular arrangement. For TPPS J-aggregates, $2J = -0.4$ eV and the field-induced red-shift energy is 1.4×10^{-5} eV. If we take, for example, $r = 1$ nm and $\theta = 20^\circ$, then the observed energy shift is caused by the change in θ as small as $\Delta\theta = 0.002^\circ$, or the change in r as small as $\Delta r = 0.0001$ Å. The change in the angle seems to be more probable than that in the distance for the following reason: The dipole moment is induced in the constituent monomers by the field, and it rotates due to the torque exerted by the field. In this case, no change occurs in the center of mass for each molecule. When the mutual distance changes, however, the monomers located on both ends of the aggregates should change its position by a much larger distance. This is unlikely to occur.

Fig. 5 depicts this model to explain the experimental finding of the electric-field dependence. Initially, i.e., before the electric field is applied, the constituent molecules in the J-aggregates are located at certain stable positions, making a finite angle between the molecular transition dipole moment and the intermolecular bonding axis, which are determined by the intermolecular interaction and the polymer potential. When an alternating electric field is applied, the electric-field induced dipole moments in the molecules

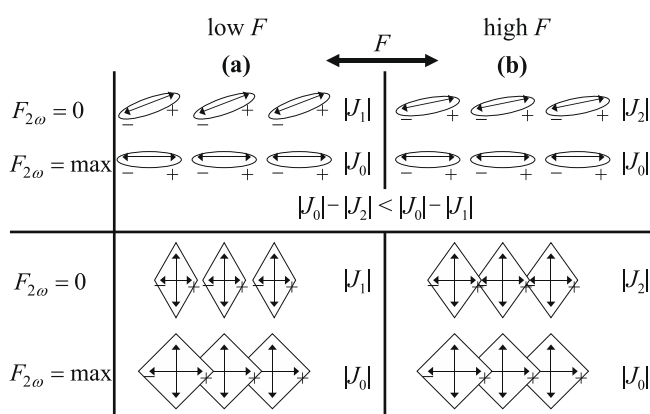


Fig. 5. Schematic of the rearrangement model. Above: (a) With ($F \neq 0$) and without ($F = 0$) electric field, each molecule in J-aggregates changes its direction such that the molecular axes are more aligned due to the electric-field induced dipole moment (expressed by + and -) in the ground state. It does not matter whether it is in the ground or excited state because there is no substantial difference in the polarizability between the two as measured for the monomer. Since $|J_1| < |J_0|$, the B-band is red-shifted by $2(|J_0| - |J_1|)$. The transition dipole moment is denoted by the thin double-sided arrows (\leftrightarrow). The direction of the applied alternating electric field is shown by the thick double-sided arrow. (b) If the electric field is large, the molecules are rearranged into the more aligned configurations with $J = J_2$ by the $F_{\omega=0}(\propto F^2)$ component to give a smaller $F_{2\omega}(\propto F^2)$ -induced red shift by $2(|J_0| - |J_2|)$. Below: more realistic model for the molecular arrangement with a slipped face-to-face stacking from top view, which takes account of the molecular structure for the diacid H_4TPPS^{2-} monomer. There are two orthogonal transition dipole moments in the molecular plane. The side view is similar to the arrangement shown in the above figure.

tend to be aligned along the electric-field direction. As a result, the angle decreases and the transition dipole–transition dipole interaction J increases, resulting in the red shift of the J-band.

The upper part of Fig. 5 shows the simplest model for a rod-like molecule, where the induced and transition dipole moments are both parallel to the molecular axis. The lower part of Fig. 5 shows a more realistic model for a disk-like TPPS molecule. The monomer constituting the aggregates is the diacid H_4TPPS^{2-} molecule such that the positively charged center of one H_4TPPS^{2-} molecule attracts the negatively charged peripheral substituents of the adjacent molecules to form a linear assembly with a slipped face-to-face stacking [19]. Since the monomer has two orthogonal transition dipole moments in the molecular plane, the assembly forms J- and H-aggregates simultaneously. The lower part shows the top view of the assembly, while the upper part is regarded as the side view in this respect. If the TPPS aggregates are isotropically distributed in the matrix, the electric-field induced shift occurs evenly in both (red and blue) directions. In the present experiment, by contrast, we used the spin-coated PVA film, under which the electrodes were deposited. Therefore, the aggregates were distributed in the film plane and the in-plane electric field was applied. This is exactly the case depicted in Fig. 6, where the red shift dominates over the blue shift in agreement with the experiment.

4.2. Electric-field dependence

The intuitive view presented above is theoretically supported by a simple mechanical model in the following. As shown in Fig. 7, monomer molecules are positioned in the mechanical equilibrium such that its molecular axis is tilted by a small angle $\theta_0 (\ll 1)$ with respect to the intermolecular bonding axis. When the alternating electric field F is applied in the direction of the bonding axis, a dipole moment is induced in the molecular axis of each monomer and is made aligned in the field direction. We assume the Lorentz model with displacement x for the induced dipole moment qx in the monomer with q being the electronic charge. This aggregate can rotate as a rigid body around its center of mass by the angle of θ with respect to θ_0 against the restoring force. Then, the equations of motion are represented by

$$m(\ddot{x} + \omega_0^2 x) = qF \cos(\theta_0 - \theta) \simeq qF, \quad (4)$$

$$I(\ddot{\theta} + \Omega_0^2 \theta) = qx F \sin(\theta_0 - \theta) \simeq qx F (\theta_0 - \theta), \quad (5)$$

where m is the mass of the charge, I is the moment of inertia for the monomer, ω_0 and Ω_0 are the resonance frequencies due to the restoring force, and $\theta_0 - \theta$ is the angle from the intermolecular bonding axis. Substituting $F = F_0 \cos \omega t$ and $x = x_0 \cos \omega t$ with $\omega = 2\pi f$ ($\omega_0, \Omega_0 \gg \omega$), we obtain

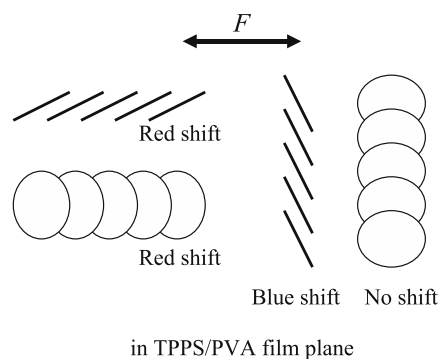


Fig. 6. Four possible directional arrangements of TPPS aggregates in the spin-coated PVA film. Any arrangement of the aggregate is expressed by the combination of these four, all of which occur at the same probability. Thus, the red shift is dominated over the blue shift when the electric field is applied in the film plane.

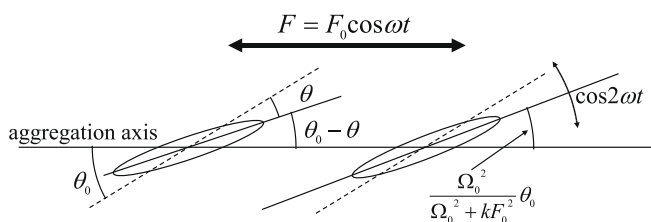


Fig. 7. Left: definition of the angles θ and θ_0 in the mechanical model for the molecular rearrangement model. The magnitude of the angles is exaggerated. Right: with $F = F_0 \cos \omega t$ applied, the axis of the monomer molecule oscillates with 2ω about the angle of $\Omega_0^2 \theta_0 / (\Omega_0^2 + kF_0^2)$ (Eq. (8)), which is decreased for larger F_0 .

$$x_0 = \frac{q}{m} \frac{F_0}{\omega_0^2 - \omega^2}, \quad (6)$$

$$xF = \frac{q}{2m} \frac{F_0^2}{\omega_0^2 - \omega^2} (1 + \cos 2\omega t) \equiv F_{\omega=0} + F_{2\omega} \cos 2\omega t. \quad (7)$$

The first term in Eq. (7) rearranges the molecular axes in a more aligned position, as shown in Fig. 5b, and the second term modulates them at $2f$. Neglecting the higher-order terms than F_0^2 , one can obtain

$$\theta_0 - \theta \simeq \frac{\Omega_0^2}{\Omega_0^2 + A} \theta_0 - \phi_0 \cos 2\omega t \quad (8)$$

$$\simeq \frac{\Omega_0^2}{\Omega_0^2 + A} \theta_0 \left(1 - \frac{A}{\Omega_0^2 + A} \cos 2\omega t \right) \quad (9)$$

with

$$A = \frac{q^2}{2ml} \frac{F_0^2}{\omega_0^2 - \omega^2} \simeq \frac{q^2}{2ml} \frac{F_0^2}{\omega_0^2} \equiv kF_0^2, \quad (10)$$

$$\phi_0 = \frac{A\Omega_0^2}{(\Omega_0^2 + A - 4\omega^2)(\Omega_0^2 + A)} \theta_0 \simeq \frac{A\Omega_0^2}{(\Omega_0^2 + A)^2} \theta_0. \quad (11)$$

Eq. (9) explains the electric-field dependence of the signal depicted in Fig. 5, as illustrated in Fig. 7. To be more precise, the F_0 dependence of the modulation of J is estimated with Eq. (3) as

$$J = \frac{M^2}{4\pi\epsilon_B r^3} (1 - 3 \cos^2(\theta_0 - \theta)) \simeq \frac{M^2}{4\pi\epsilon_B r^3} [-2 + 3(\theta_0 - \theta)^2] \quad (12)$$

with

$$(\theta_0 - \theta)^2 = -2 \frac{\Omega_0^2}{\Omega_0^2 + A} \phi_0 \theta_0 \cos 2\omega t + C, \quad (13)$$

$$\simeq -2 \frac{k\Omega_0^4 F_0^2}{(\Omega_0^2 + kF_0^2)^3} \theta_0^2 \cos 2\omega t + C, \quad (14)$$

$$\simeq -2 \frac{kF_0^2}{\Omega_0^2 + 3kF_0^2} \theta_0^2 \cos 2\omega t + C, \quad (15)$$

where C represents terms other than that oscillating with 2ω and the minus sign indicates the red shift in the J band. For order estimation, A is roughly estimated to be 10^{19} s^{-2} when ω_0 is of the electronic origin such that $\omega_0 \sim 10^{15}$, q is taken as the charge of the electron and m as its mass, l is taken as $10 \times (\text{proton mass}) \times (1 \text{ \AA})^2$, and $F_0 \sim 10^6 \text{ V/m}$. If Ω_0 is in the range of GHz, as is reasonable for the rotational frequency, A ($\equiv kF_0^2$) and Ω_0^2 are comparable in Eq. (15), resulting in a deviation from the F_0^2 dependence of the $2f$ signal intensity (red shift in the J band), as observed in Fig. 2a.

As for the monomer, by contrast, the electric-field dependent energy is expressed simply by

$$E = -qx F \cos(\theta_0 - \theta) \simeq -qx F \simeq -\frac{q^2 F_0^2}{2m\omega_0^2} (1 + \cos 2\omega t). \quad (16)$$

This is purely the electronic response without a saturation effect. Although there is a contribution from the molecular rotation to the polarizability as well, it is readily deduced that the rotational

contribution is of higher order than F_0^2 such that the electronic contribution dominates for the $2f$ response.

4.3. Frequency dependence

The modulation-frequency dependence is more difficult to explain. As shown in Fig. 4, there are three patterns: as the frequency is increased, the ratio of $\Delta\alpha_{\text{agg}}$ to $\Delta\alpha_{\text{mon}}$ decreases in Fig. 4a, increases in Fig. 4b, and initially decreases steeply and gets leveled in Fig. 4c, while $\Delta\alpha_{\text{mon}}$ stays nearly constant in the whole frequency range in Fig. 4d. It is unknown what experimental parameters and what conditions for sample preparation determine the frequency dependence, but one of the possible explanations is as follows.

The observations in Fig. 4a can be explained by the change in the local-field behavior due to the frequency-dependent dielectric constant ϵ of a PVA matrix. A hydrophilic-polymer film like PVA contains moisture in highly humid environment. When many water molecules enter into main polymer chains, interaction between the chains is reduced and its dielectric constant ϵ increases more for lower frequencies, say between 10^1 and 10^4 Hz [18]. The frequency dependence of ϵ for a moistened PVA film was measured in this frequency range, as shown in Fig. 8. From Eq. (1), the local field decreases as ϵ decreases with frequency. As a result, the signal intensity decreases with frequency as shown in Fig. 4a. One of the drawbacks for this mechanism is that the frequency dependence for the monomer should also have been observed for this reason. In addition, the behavior in Fig. 4b and c is left to be explained.

4.4. Coupling model with charge-transfer states

Our final remark is concerned with a possible contribution from the CT states to the enhancement in the $\Delta\alpha$ for J-aggregates. Coupling between the Frenkel and CT excitations, which is proposed to be responsible for the difference in the polarizability between the excited and ground states, has been used to account for the electroabsorption spectra in polyacene crystals [12–14]. In the present experiment, there exists one characteristic feature which cannot be explained by the rearrangement model. As seen in Fig. 1, the ΔA spectrum for J-aggregates is not fit completely by the first derivative of the absorption spectrum, but there is a residual feature around 2.46 eV, i.e., a small negative peak showing a decrease in the absorption. This might be a signature of the CT states which emerges if the wavefunctions of neighboring molecules overlap spatially.

The model Hamiltonian for dimer molecules in Ref. [12] can be used to obtain some insight into the possible contribution of the CT states to the difference in the polarizability observed here.

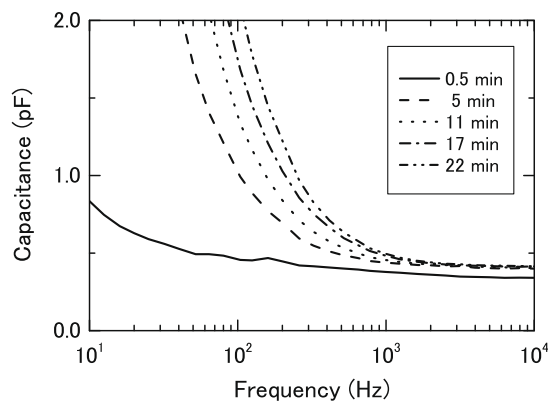


Fig. 8. Frequency dependence of the capacitance of a PVA film as a function of the elapsed time after it was placed in highly humid (100%) circumstances.

$$\begin{pmatrix} E_{F+} & D_+ & 0 & 0 \\ D_+ & E_{CT+} & -pF & 0 \\ 0 & -pF & E_{CT-} & D_- \\ 0 & 0 & D_- & E_{F-} \end{pmatrix} = \begin{pmatrix} 2.52 & 0.01 & 0 & 0 \\ 0.01 & 2.46 & -0.002 & 0 \\ 0 & -0.002 & 2.525 & 0.01 \\ 0 & 0 & 0.01 & 2.8 \end{pmatrix}, \quad (17)$$

where E_{F+} and E_{F-} are the Frenkel exciton energies for symmetric and antisymmetric combinations of the locally excited states, respectively ($|AB^+\rangle \pm |A^*B\rangle$), and E_{CT+} and E_{CT-} are the CT exciton energies for symmetric and antisymmetric combinations of the charged states, respectively ($|A^-B^+\rangle \pm |A^+B^-\rangle$). D_+ and D_- denote the coupling energies between the Frenkel and CT states, and p is the dipole moment of the CT states, and F is the static electric field. The E_{F+} exciton is optically allowed, while the E_{F-} exciton is optically forbidden. The CT excitons have negligible oscillator strengths in comparison with the Frenkel excitons.

The values for E_{F+} and E_{CT+} [eV] are taken from the B band absorption peak and the negative peak in the ΔA spectrum, respectively. E_{CT-} [eV] is assumed to be located slightly above the E_{F+} , in order to induce a significant red shift by F as a result of repulsion between closely spaced E_{F+} and E_{CT-} states. E_{F-} [eV] is taken to be sufficiently distant from E_{F+} , reflecting the large J , but it does not precisely follow the experimental value since this is the dimer model different from the real situation for the J-aggregates. p is assumed to be $e \times 1$ nm with e being the charge of the electron, i.e., one electron is moved between the molecules separated by 1 nm. The values for D_+ and D_- [eV] are taken from Ref. [14]. Then, the above matrix is numerically diagonalized both for $F = 0$ and $F = 2 \times 10^6$ V/m as follows:

$$\begin{pmatrix} E_{F+}^0 \\ E_{CT+}^0 \\ E_{CT-}^0 \\ E_{F-}^0 \end{pmatrix} = \begin{pmatrix} 2.52162 \\ 2.45838 \\ 2.52464 \\ 2.80036 \end{pmatrix} \quad (18)$$

for $F = 0$, and

$$\begin{pmatrix} E_{F+}^F \\ E_{CT+}^F \\ E_{CT-}^F \\ E_{F-}^F \end{pmatrix} = \begin{pmatrix} 2.52159 \\ 2.45832 \\ 2.52473 \\ 2.80036 \end{pmatrix} \quad (19)$$

for $F = 2 \times 10^6$ V/m.

The E_{F+}^0 state red-shifts to E_{F+}^F by 3×10^{-5} eV in reasonable agreement with the experiment, and the E_{CT+}^0 state decreases its oscillator strength to give the E_{CT+}^F state: For $F = 0$, the E_{CT+} state acquires the oscillator strength by coupling with the optically allowed E_{F+} state alone, and for $F \neq 0$, it decreases the oscillator strength by coupling not only with the E_{F+} state but also with the E_{CT-} state. This simple model shows the possibility that coupling between the Frenkel and CT excitons is the origin of the large difference in the polarizability observed for the J-aggregates.

However, this model needs further theoretical refinement. First, this is a simplified model, where only the dimer is considered. Second, the energy positions for both E_{CT+} and E_{CT-} states need to be theoretically justified. It is artificially assumed here, to reproduce the experimental observation, that E_{CT+} is only slightly below E_{F+} and that E_{CT-} is at nearly the same level as E_{F+} . Third, this model

can hardly explain the deviation from the quadratic dependence of the signal on the electric-field strength.

5. Conclusion

We have found a deviation from the quadratic dependence of the Kerr signal intensity on the electric field for TPPS J-aggregates. This behavior is characteristic of J-aggregates and is not observed for monomers. The modulation frequency dependence has also been observed only for J-aggregates, and it has three typical patterns. These unique features can be explained qualitatively by the molecular rearrangement model proposed in the present study. This model is quantitatively reasonable as well: The observed large enhancement in $\Delta\alpha$ accompanying aggregate formation is shown to be caused by an angular rearrangement as small as 0.002° of the constituent molecules in response to the applied electric field.

In comparison, we have examined the validity of the coupling model of charge-transfer and Frenkel excitations: The enhancement in $\Delta\alpha$ can be explained quantitatively. In addition, the residual feature at 2.46 eV in Fig. 1 can be explained qualitatively, although the signal intensity has not been evaluated quantitatively. Nor is it possible to explain the non-quadratic dependence on the electric field, so that it needs further theoretical refinement.

The rearrangement model is therefore considered to be as appropriate as the conventional coupling model for explaining the electrooptic response in porphyrin J-aggregates. In order to give a further experimental support to this model, one needs to study samples with orientational order of the aggregates other than that in a spin-coated film or another geometry of the applied electric field direction with respect to the sample.

Acknowledgements

The authors thank T. Furukawa and Y. Takahashi, in the Department of Chemistry, Tokyo University of Science, for their measurements of the frequency dependence of the dielectric constant of PVA films.

References

- [1] T. Ogawa, E. Tokunaga, T. Kobayashi, Chem. Phys. Lett. 408 (2005) 186.
- [2] K. Misawa, T. Kobayashi, Nonlinear Optics 14 (1995) 103.
- [3] H. Wendt, J. Friedrich, Chem. Phys. 210 (1996) 101.
- [4] T. Kobayashi, Mol. Cryst. Liq. Cryst. 314 (1998) 1.
- [5] O. Ohno, Y. Kaizu, H. Kobayashi, J. Chem. Phys. 99 (1993) 4218.
- [6] N.C. Maiti, S. Mazumdar, N. Periasamy, J. Phys. Chem. 99 (1995) 10708.
- [7] N.C. Maiti, S. Mazumdar, N. Periasamy, J. Phys. Chem. 102 (1998) 1528.
- [8] T. Kobayashi, T. Saito, C. Hikage, K. Misawa, Meeting Abstracts Phys. Soc. Japan 53 (1998) 221.
- [9] K. Misawa, T. Kobayashi, Technical Digest of IQEC'98, 1998, p. 99.
- [10] A.S.R. Koti, J. Taneja, N. Periasamy, Chem. Phys. Lett. 375 (2003) 171.
- [11] A. Eilmes, Chem. Phys. Lett. 347 (2001) 205.
- [12] P. Petelenz, Organ. Electron. 5 (2004) 115.
- [13] M. Slawik, P. Petelenz, J. Chem. Phys. 111 (1999) 7576.
- [14] P. Petelenz, M. Slawik, Chem. Phys. 157 (1991) 169.
- [15] N. Ishii, E. Tokunaga, S. Adachi, T. Kimura, H. Matsuda, T. Kobayashi, Phys. Rev. A 70 (2004) 023811.
- [16] W. Liptay, in: E.C. Lim (Ed.), Excited States, Academic Press, New York, 1974, p. 129.
- [17] T. Kobayashi, J-Aggregates, World Scientific, Singapore, 1996.
- [18] Y. Yada, Electrical Properties of Polymers, Shokabo, Tokyo, 1987 (in Japanese).
- [19] D.M. Chen, T. He, D.F. Cong, Y.H. Zhang, F.C. Liu, J. Phys. Chem. A 105 (2001) 3981.